Metal Organic Framework-Derived Cobalt Dicarboxylate as a High-Capacity Anode Material for Lithium-ion Batteries

Liping Wang,*[a] Mingjuan Zhao,[a] Jiliang Qiu,[a] Peng Gao,[b] Jing Xue,[a] and Jingze Li*[a, c]

Considerable attention has been paid to metal-organic frameworks (MOFs) for applications as electrode materials for lithium-ion batteries recently. In this study, we use cobalt terephthalate $CoC_8H_4O_4$ (CoTPA), one type of MOFs, as an anode material for lithium-ion batteries for the first time. It delivers a high discharge capacity of about 700 mAh g^{-1} after 100 cycles with superior capacity retention. In contrast to the conventional lithium-storage mechanism of MOF-based anodes in organic carbonyl units, both the inorganic unit (Co^{2+}) and the organic unit (carbonyl group) offer multi-electron transfer reactions, which results in such a high capacity.

Introduction

Metal organic frameworks (MOFs) first reported by Yaghi and co-workers received a large amount of attention in the past two decades due to their high porosity, structural diversity, and tunable physicochemical properties.[1,2] These materials consist of inorganic units and organic units forming frameworks by strong bonds. Until now, more than 20000 MOFs have been produced, taking advantage of the diversity of inorganic and organic moieties, and the number is still growing. In addition to the application in gas storage, catalysis, sensors, proton conductor, and drug delivery, they also give rise advances in energy storage and conversion systems, especially lithium-/sodium-ion batteries.[3–5] Férey et al. first reported that lithium can be inserted/de-inserted into MOF cathodes $[Li_xFe^{II}_xFe^{III}_{1-x}(OH)_{0.8}F_{0.2}O_2C_6H_4CO_2]$ at ~3.0 V versus Li^+/Li^0 with a capacity of 75 mAh g^{-1}.[6] The MOF consisting of Zn_4O tetrahedrons and 1,3,5-benzenetribenzoate as linkers (MOF-177) was the first to be used as an anode for lithium-ion batteries but showed very poor cycling performance.[7] From an application point of view, reported MOF cathodes [e.g., MIL-53 (Fe),[6] Prussian-blue analogues,[8] and $K_{2.5}(VO)_2(HPO_4)_2(C_2O_4)$[9]] normally show a relatively low capacity of less than 100 mAh g^{-1} and MOF anodes (e.g., MOF-177,[7] $Zn_3(HCOO)_6$,[10] Na-1,4-benzenedicarboxylates (NaBDC),[11] and Ni-1,4,5,8-naphthalenetetracarboxylates (Ni-NTC)[12]) showed poor capacity retention. Thus, it is important to design MOF electrode materials with high capacity and good cyclability.

Understanding the lithium storage mechanism is essential to design new materials and modify their physicochemical properties. As for the reported MOF cathodes mentioned above, mixed valence in transition-metal compounds (Fe^{2+}/Fe^{3+}, V^{3+}/V^{2+}, Cr^{3+}/Cr^{4+} among others) are used concomitantly with lithium insertion/desertion under conditions that preserve the frameworks, which is analogous to the conventionally used inorganic cathode material $LiCoO_2$. With regard to the MOF anodes, either the inorganic moiety or the organic moiety is exploited for lithium-storage active sites. The inorganic components (e.g., Zn^{2+} and Cu^{2+}) undergo alloying or conversion reactions with lithium for high capacities whereas the organic components that are usually contain carbonyl groups undergo enolization reactions. As for the latter, this can also be extended to organic chemistry community by simply using the carbonyl groups to absorb Li or Na ions.[13–15] Wu et al. analyzed the storage mechanism of carbonyl function groups in MOF electrodes using $Na_2C_6H_4O_4$, which consists of alternating Na–O octahedral inorganic layers and π-stacked benzene layers, as a model, revealing that the Na–O inorganic layer provides Na^+ transport channels and storage sites while the organic part offers electronically active centers.[16] Recently, Lee et al. made use of the inorganic and the organic moieties in transition-metal terephthalates (NiTP, FeTP), obtaining a reversible capacity of approximately 1100 mAh g^{-1} with decent capacity retention behavior.[17]

We recently investigated the lithium/sodium storage behavior in metal terephthalates MTP (M = Li, Ca, Mg, Ag, Sr, Ba) in terms of electrochemical properties and structure–

[a] Dr. L. Wang, M. Zhao, J. Qiu, J. Xue, Prof. J. Li
State Key Laboratory of Electronic Thin Films and Integrated Devices
University of Electronic Science and Technology of China
Chengdu 610054 (PR China)
lijingze@uestc,edu.cn
E-mail: lipingwang@uestc.edu.cn

[b] Prof. P. Gao
School of Physics
Peking University
Beijing 100871 (PR China)

[c] Prof. J. Li
State Key Laboratory of Polymer Materials Engineering
Sichuan University
Chengdu 610065 (PR China)

property elucidation.[18–23] Their capacities are only attributed to the carbonyl groups, which means that the inorganic moieties are electrochemically inert. In this study, we introduce an inorganic component that participates in the energy storage into the terephthalates. Accordingly, cobalt terephthalate ($CoC_8H_4O_4$, also denoted as CoTPA) is synthesized and first applied as an anode material for lithium-ion batteries. A high capacity of more than 600 mAh g^{-1} with good cycling performance is realized through multi-electron reactions. Its lithium-storage mechanism is also studied.

Results and Discussion

Figure 1a shows the XRD patterns of cobalt terephthalate powders with and without crystal water. The XRD pattern of CoTPA·2H_2O is indexed to a monoclinic structure with a space group of *C*2/*c* (JCPDF card No. 34-1896). The lattice parameters are $a = 18.255$ Å, $b = 6.536$ Å, $c = 7.289$ Å, and $\beta = 98.64°$ based on a profile-matching mode using the Fullprof-suite software,[24] which is consistent with the results reported by Hall and other authors.[25,26]

After heat treatment at 350 °C for 6 h under Ar/H_2 atmosphere, anhydrous CoTPA powders with blue color were obtained. The structure of cobalt terephthalate, to the best of our knowledge, is unknown, but its crystal structure seems to be less stable compared with the CoTPA·2H_2O powders, a sign of grain-size decrease or amorphization. According to TGA analysis (Figure 1b), CoTPA contains two water molecules in the crystal per formula unit. The crystallographic structure of CoTPA·2H_2O at [010] and [001] directions are presented in Figure 1c and d, respectively. This structure consists of octahedral Co–O inorganic layers parallel to the *bc* plane and terephthalate organic layers parallel to the *ab* plane. The inorganic–inorganic and organic–organic layer distances are 9.13 and 3.64 Å, respectively, and the angle for the two planes is 67.0°. The carbonyl groups in CoTPA·2H_2O with a C=O bond length of 1.230 Å and a C–O bond length of 1.289 Å are conjugated, which is common in terephthalates.[27]

The synthesis of MTPA (M = Li, Ca, Mg) powders in aqueous solution even at room temperature can easily lead to the formation of micrometer-sized particles, which demonstrates that the formation energy for MTPA is comparatively low.[20,22] In our case, as-obtained CoTPA·2H_2O has an average particle size of 1–2 μm (Figure 2a). Consistent with the XRD study shown in Figure 1a, the smooth surface of the large rock-like particles suggests a high crystallinity. After dehydration, the particle sizes of the resultant CoTPA are much smaller, decreasing to sub-micrometer size (Figure 2b). Loss of crystal water easily produces smaller particle sizes

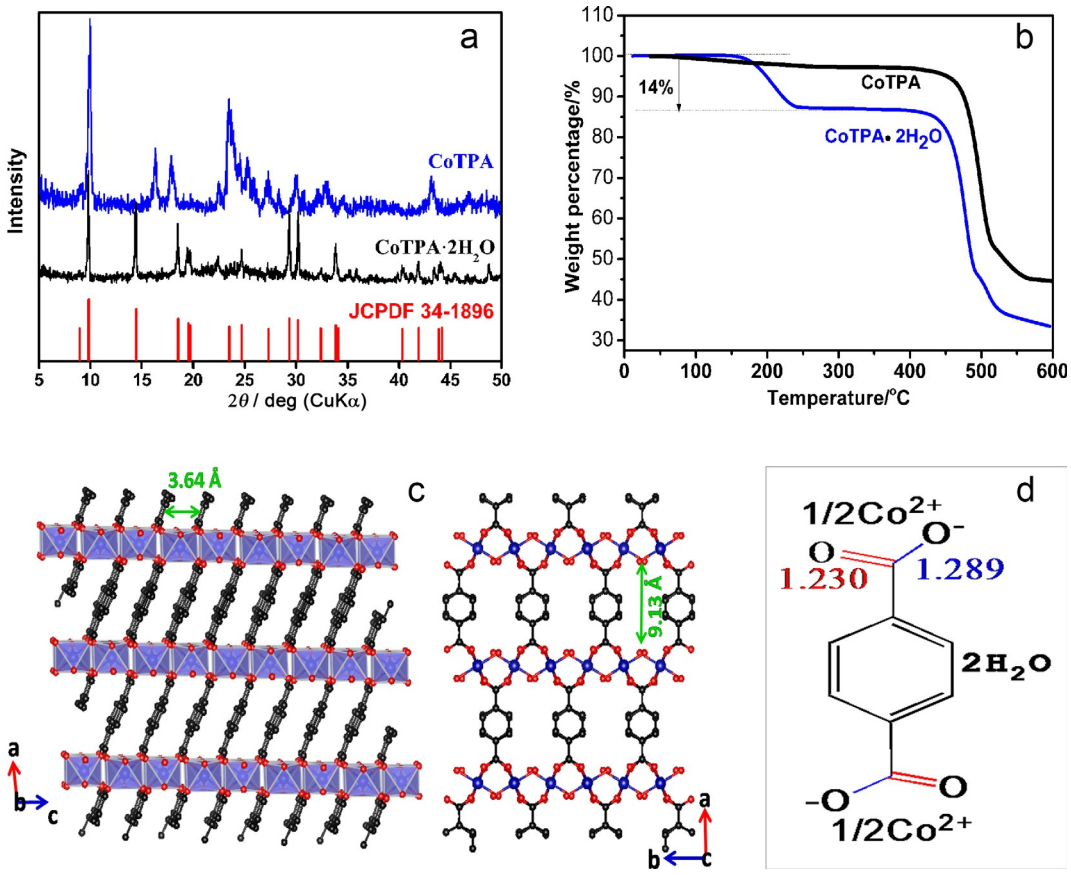

Figure 1. a) XRD patterns of CoTPA·2H_2O and CoTPA powders, b) thermogravimetric analysis (TGA) curves of hydrous and anhydrous CoTPA, c) projection of the crystal structure of CoTPA·2H_2O along the *b*- and *c*-axis. The O, Co, and C atoms are shown as red, blue, and black balls, respectively; H atoms are omitted. d) Molecular structure of CoTPA·2H_2O including bond lengths.

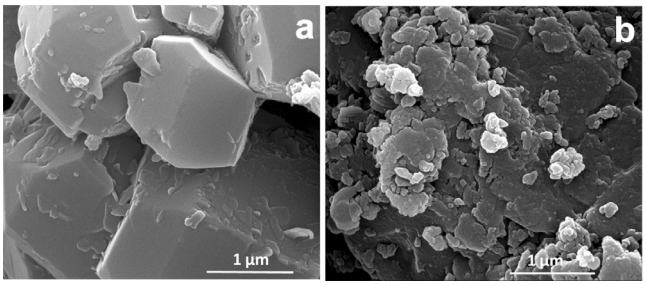

Figure 2. SEM images of a) CoTPA·2 H_2O and (b) CoTPA.

and cracks owing to a phase transition or volume expansion/contraction occurring during dehydration.[20] The electrochemical properties of CoTPA were evaluated using CoTPA/Li half cells. Figure 3a depicts the cyclic voltammetry of CoTPA at a scan rate of 0.05 mV s^{-1} in the voltage window 0.005–2.8 V whereas the first three galvanostatic charge–discharge curves at a current density of 60 mA g^{-1} are displayed in Figure 3b. In the first cathodic process, a reduction peak at 1.1 V (accounting for a capacity of ~280 mAh g^{-1}) is observed. Assuming about 2 mol electrons transferred per molecular weight for this step and an operational voltage of Co^{2+}/Co^0 versus Li^+/Li^0 (e.g., CoO[28,29]), we suggest that CoTPA reacts with Li according to the following reaction: $CoTPA + 2Li^+ + 2e^- \rightarrow Li_2TPA + Co$. The second reduction peak located at ~0.7 V is a characteristic for the enolization of carbonyl group in metal terephthalates.[30] The reaction is described as follows: $Li_2TPA + 2Li^+ + 2e^- \rightarrow Li_4TPA$. Discharged from 0.5 to 0.005 V, a sloped curve corresponding to a capacity of 200 mAh g^{-1} is observed for the second cycle; we believe that the lithium is inserted into the benzene ring according to the reaction of $Li_4TPA + xLi^+ + xe^- \rightarrow Li_{4+x}TPA$, as it was reported that lithium ions can be inserted into a fused C_6 aromatic ring by Sun's group.[31] Recently, Alam and Manzhos[32] revealed that a part of capacity of sodium teraphthalate could be ascribed to the hexagonal sites of the benzene ring. Interestingly, CoTPA has an excellent capacity retention at a current density of 60 mA g^{-1} in the voltage window 0.005–2.8 V (Figure 3c). The initial discharge capacity is 1938 mAh g^{-1} followed by a reversible charge capacity of 1004 mAh g^{-1}. This initial coulombic efficiency (51.8%) is low compared with commercial anodes, such as graphite and $Li_4Ti_5O_{12}$, but common in organic electrodes and carbon-based materials.[33,34] This low efficiency is partly related to the decomposition of carbon-based organic electrolyte at low voltage and/or formation of an solid electrolyte interphase (SEI), irreversible bonding of Li^+ ions onto the aromatic structure as well as voltage hysteresis occurring during the conversion reaction due to poor kinetics and the presence of phase boundaries.[35,36] This drawback can be principally improved by replacement of electrochemi-

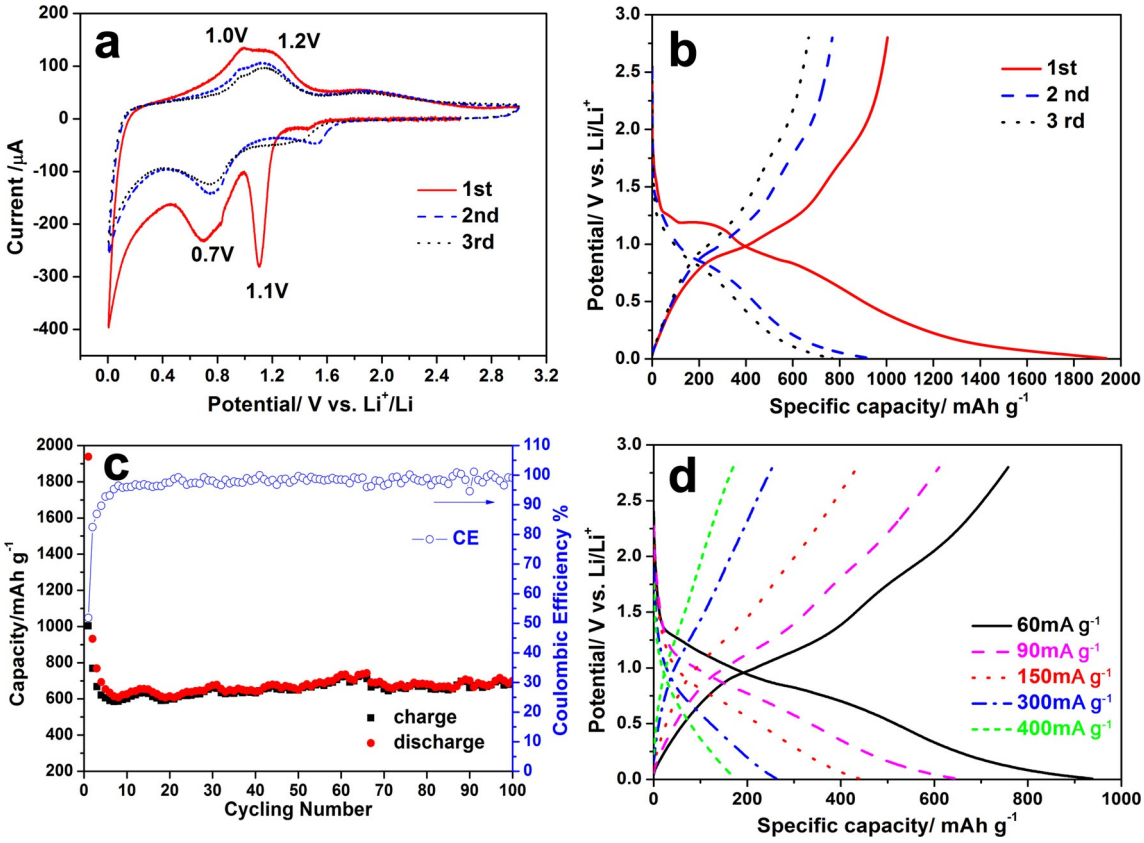

Figure 3. a) Cyclic voltammetry curves of CoTPA at a scan rate of 0.05 mV s^{-1} and b) the galvanostatic charge–discharge curves of CoTPA at a current density of 60 mA g^{-1} in the voltage window 0.005–2.8 V for the first three cycles; c) capacity retention behavior as a function of cycling number at a constant charge–discharge rate of 60 mA g^{-1}, and d) rate performance of CoTPA at various current densities

cally stable electrolytes such as ionic liquids and addition of highly conductive additives for better kinetics. Note that the coulombic efficiency is stable after the first several cycles. The discharge capacity of 606 mAh g^{-1} for the fifth cycle increases to 692 mAh g^{-1} for the 107th cycle, which demonstrates an activation process in the anode material. The rate performance is also good (Figure 3d), showing a discharge capacity of 937, 645, 443, 264, and 175 mAh g^{-1} at a current density of 60, 90, 150, 300, and 400 mA g^{-1}, respectively. Such electrochemical properties in terms of capacity and capacity retention behavior are extremely good. The capacity is two or three times higher than the well-known Li_2TPA reported by Armand et al.[30] and CaTPA in our former study.[19] This is comparable to a recent publication by Lee et al., who used NiTP and FeTP as anodes with a high capacity for lithium-ion batteries.[17] Moreover, we believe that the electrochemical properties of the obtained CoTPA can be optimized by minimizing the particle size and/or coating highly electron-conductive materials.

To further elucidate and prove our proposed electrochemical reaction mechanism, TEM, XRD, and FTIR experiments were performed for tracking the structural changes at various charge–discharge states (Figure 4). Figure 4a and b shows the structure and morphology of CoTPA at a discharge state of 0.005 V. It is found that metallic Co (JCPDF No. 15-0806) particles formed and were well dispersed in the discharged matrix, which confirms that the Co^{2+} in CoTPA takes part in the electrochemical reaction and is reduced to Co^0. In addition, its discharged morphology has amorphous features, indicating that the insertion of Li could corrupt the crystal structure, which is consistent with the study of Wang et al.[37] Also, the weak and broad diffraction peaks of metallic Co presenting CoTPA at a discharge state of 0.005 V (Figure 4c) reveals that the electrochemically formed Co particles are small, even smaller than the coherence length of X-rays. All the information obtained from the XRD measurement is consistent with the TEM study. In the Fourier-transform infrared (FTIR) spectrum of cobalt terephthalate anhydrate shown in Figure 4d, there are stretching bands at 1605 and 1397 cm^{-1}, which are assigned to ν_{as}(COO) and ν_s(COO), respectively. The characteristic peak of δ_{Co-O} at 548 cm^{-1}, which is blue-shifted to 561 cm^{-1} after discharge to 1.0 V, suggests replacement of Co^{2+} ions by Li^+ ions. After a discharge–charge cycle, the molecular structure of CoTPA is almost preserved, which is in accordance with the results of Li et al.,[38] who demonstrate the electrochemical reversibility of the Co^{2+}/Co interconversion and the stability of their electronic structure (confirmed by X-ray photoelectron spectroscopy together with an electron paramagnetic resonance measurement). All of these evidences confirm our proposed reaction mechanisms for the CoTPA materials.

Conclusions

In this study, one type of metal-organic framework (MOF), namely cobalt terephthalate (CoTPA), was synthesized and applied as an anode material of lithium-ion batteries for the first time. It presents an operational voltage below 1.2 V vs. Li^+/Li^0 with a high discharge capacity of more than 600 mAh g^{-1}. The capacity retention behavior improves after an activation process, and the capacity increases to about 700 mAh g^{-1} after 100 cycles. It is found that both the inor-

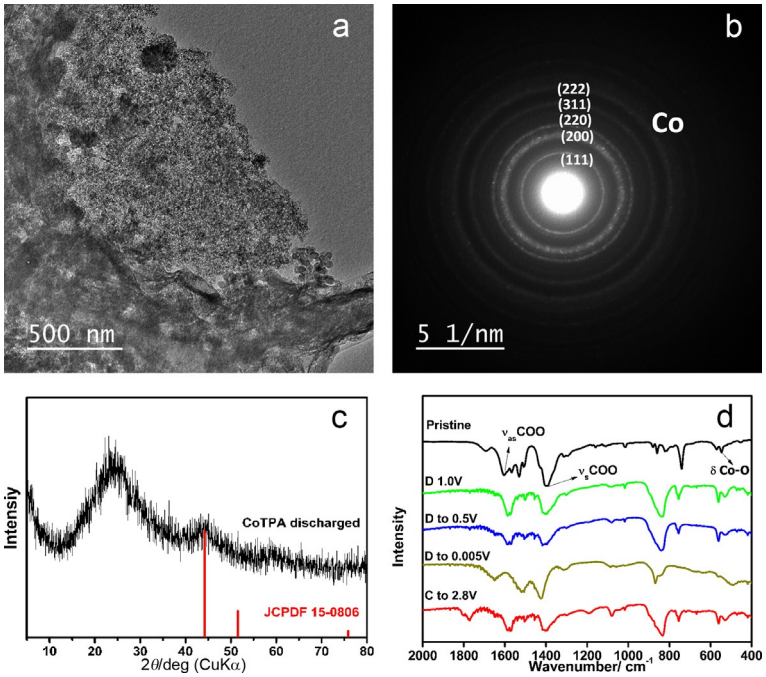

Figure 4. a) TEM images and b) selected-area electron diffraction (SAED) patterns and c) XRD patterns (including the Co pattern for reference) of CoTPA discharged to 0.005 V, and d) FTIR spectra of CoTPA at various charge (C)–discharge (D) states.

ganic unit (Co^{2+}) and the organic unit (carbonyl group and aromatic structure) have electronically active sites for lithium storage. This multi-electron transfer reaction-based material with a high capacity and good capacity retention behavior may bring new perspectives in exploring new MOF materials and applications in other energy-storage systems.

Experimental Section

Material synthesis

All chemicals were of analytical grade and used as received without further purification. Similar to the preparation of calcium terephthalate (CaTPA) reported in our previous study,[19–21] cobalt terephthalate (CoTPA) was synthesized by a displacement reaction between di-lithium terephthalate and cobalt dichloride hexahydrate. Typically, 0.02 mol $LiOH{\cdot}H_2O$ and 0.01 mol *p*-phthalic acid were dissolved in 100 mL deionized water while stirring continuously for 6 h. Afterwards, 0.01 mol cobalt dichloride hexahydrate solution was added dropwise to the transparent solution, resulting in the formation of cobalt terephthalate hydrate as pink precipitate at 80 °C. The precipitate were centrifuged and washed with deionized water and ethanol several times to obtain $CoTPA{\cdot}2H_2O$. For the preparation of anhydrous CoTPA, the obtained $CoTPA{\cdot}2H_2O$ was heated to 350 °C at a heating rate of 5 °C min^{-1} under Ar/H_2 atmosphere and the temperature was held for 6 h. After cooling to room temperature, CoTPA powders with blue color were obtained.

Material characterization

X-ray diffraction patterns for crystal structures were collected using a Philips X'Pert MPD (40 kV/100 mA) diffractometer (λ = 1.54056 Å). Each pattern was recorded in the range of 5–80° (2θ) with a step size of 0.03°. The morphologies of $CoTPA{\cdot}2H_2O$ and CoTPA powders were investigated by a field-emission scanning electron microscope (FE-SEM, Hitachi S3400N). Thermo-gravimetric analysis (TGA, TA instrument Q500) was performed to evaluate the thermal stability of the powders and the number of crystal water molecules per formula unit; samples were heated under nitrogen atmosphere at a heating rate of 10 °C min^{-1} from RT to 600 °C. TEM experiments were carried out at 200 kV using a JEOL 2100F microscope. Infrared spectra were recorded from KBr pellets in the range 4000–400 cm^{-1} by using a SHIMADZU FT-IR 8400.

Cell assembly and electrochemical tests

For the electrochemical measurements, the electrodes were prepared by casting a slurry of 60 wt% active material, 30 wt% carbon black, and 10 wt% polyvinylidene fluoride (PVDF) binder on Cu foil. CoTPA electrodes were dried in vacuum at 110 °C for 12 h. Lithium foil and polypropylene (PP) membrane (Celgard 2400) were used as the anode and the separator, respectively. The electrolyte consisted of 1 M $LiPF_6$ dissolved in a mixture of ethylene carbonate (EC) and dimethyl carbonate (DMC) (1:1 by volume). Swagelok-type cells were assembled in an Ar-filled glove box and cycled between 0.005 and 2.8 V at current densities ranging from 60 to 400 mA g^{-1} using a CT2001 A cell test instrument (LAND Electronic Co.). Cyclic voltammetry (CV) curves were performed at a scan rate of 0.05 mV s^{-1} using a Solartron SI1287 electrochemical workstation. All the measurements were carried out at room temperature. The weight of the active materials was 1–2 g cm^{-2}.

Acknowledgements

This work is supported by the National Science Foundation of China (51502032, 21673033, 11234013, 21473022), the Science and Technology Bureau of Sichuan Province of China (no.2015HH0033), Fundamental Research Funds for the Central Universities, China (ZYGX2012Z003), and the Opening Project of State Key Laboratory of Polymer Materials Engineering (Sichuan University) (Grant No. Sklpme2016-4-23)

Keywords: batteries · carboxylate · cobalt · lithium · metal organic frameworks

[1] H. Furukawa, K. E. Cordova, M. O'Keeffe, O. M. Yaghi, *Science* **2013**, *341*, 974–986.
[2] O. M. Yaghi, M. O'Keeffe, N. W. Ockwig, H. K. Chae, M. Eddaoudi, *Nature* **2003**, *423*, 705–714.
[3] X.-M. Lin, T.-T. Li, Y.-W. Wang, *Chem. Asian J.* **2012**, *7*, 2796–2804.
[4] X.-W. Liu, T.-J. Sun, J.-L. Hu, S.-D. Wang, *J. Mater. Chem. A* **2016**, *4*, 3584–3616.
[5] L. Wang, Y. Han, X. Feng, J. Zhou, P. Qi, B. Wang, *Coord. Chem. Rev.* **2016**, *307*, 361–381.
[6] G. Férey, F. Millange, M. Morcrette, C. Serre, M. L. Doublet, J. M. Grenèche, J. M. Tarascon, *Angew. Chem. Int. Ed.* **2007**, *46*, 3259–3263; *Angew. Chem.* **2007**, *119*, 3323–3327.
[7] X. Li, F. Cheng, S. Zhang, J. Chen, *J. Power Sources* **2006**, *160*, 542–547.
[8] Y. You, X.-L. Wu, Y.-X. Yin, Y.-G. Guo, *Energy Environ. Sci.* **2014**, *7*, 1643–1647.
[9] M. Nagarathinam, K. Saravanan, E. J. H. Phua, M. v. Reddy, B. V. R. Chowdari, J. J. Vittal, *Angew. Chem. Int. Ed.* **2012**, *51*, 5866–5870; *Angew. Chem.* **2012**, *124*, 5968–5972.
[10] K. Saravanan, M. Nagarathinam, P. Balaya, J. J. Vittal, *J. Mater. Chem.* **2010**, *20*, 8329–8335.
[11] A. Abouimrane, W. Weng, H. Eltayeb, Y. J. Cui, J. Niklas, O. Poluektov, K. Amine, *Energy Environ. Sci.* **2012**, *5*, 9632–9638.
[12] X. Han, F. Yi, T. Sun, J. Sun, *Electrochem. Commun.* **2012**, *25*, 136–139.
[13] H. Chen, M. Armand, G. Demailly, F. Dolhem, P. Poizot, J. M. Tarascon, *ChemSusChem* **2008**, *1*, 348–355.
[14] Z. Song, H. Zhou, *Energy Environ. Sci.* **2013**, *6*, 2280–2301.
[15] C. Luo, R. M. Huang, R. Kevorkyants, M. Pavanello, H. X. He, C. S. Wang, *Nano Lett.* **2014**, *14*, 1596–1602.
[16] X. Wu, S. Jin, Z. Zhang, L. Jiang, L. Mu, Y.-S. Hu, H. Li, X. Chen, M. Armand, L. Chen, *Sci. Adv.* **2015**, *1*, e1500330.
[17] H. H. Lee, Y. Park, S. H. Kim, S. H. Yeon, S. K. Kwak, K. T. Lee, S. Y. Hong, *Adv. Funct. Mater.* **2015**, *25*, 4859–4866.
[18] H. Zhang, Q. Deng, A. Zhou, X. Liu, J. Li, *J. Mater. Chem. A* **2014**, *2*, 5696–5702.
[19] L. Wang, H. Zhang, C. Mou, Q. Cui, Q. Deng, J. Xue, X. Dai, J. Li, *Nano Res.* **2015**, *8*, 523–532.
[20] L. Wang, C. Mou, Y. Sun, W. Liu, Q. Deng, J. Li, *Electrochim. Acta* **2015**, *173*, 235–241.
[21] C. Mou, L. Wang, Q. Deng, Z. Huang, J. Li, *Ionics* **2015**, *21*, 1893–1899.
[22] Z. L. Huang, L. P. Wang, C. X. Mou, J. Z. Li, *Acta Phys. Chim. Sin.* **2014**, *30*, 1787–1793.
[23] L. Wang, C. Mou, B. Wu, J. Xue, J. Li, *Electrochim. Acta* **2016**, *196*, 118–124.
[24] L. P. Wang, H. Li, X. J. Huang, E. Baudrin, *Solid State Ionics* **2011**, *193*, 32–38.

[25] S. R. Hall, F. H. Allen, I. D. Brown, *Acta Crystallogr. Sect. A* **1991**, *47*, 655–685.
[26] J. A. Kaduk, *Acta Crystallogr. Sect. B* **2002**, *58*, 815–822.
[27] D. Banerjee, J. B. Parise, *Cryst. Growth Des.* **2011**, *11*, 4704–4720.
[28] P. Poizot, S. Laruelle, S. Grugeon, L. Dupont, J. Tarascon, *Nature* **2000**, *407*, 496–499.
[29] S. Xiong, J. S. Chen, X. W. Lou, H. C. Zeng, *Adv. Funct. Mater.* **2012**, *22*, 861–871.
[30] M. Armand, S. Grugeon, H. Vezin, S. Laruelle, P. Ribiere, P. Poizot, J. M. Tarascon, *Nat. Mater.* **2009**, *8*, 120–125.
[31] X. Han, G. Qing, J. Sun, T. Sun, *Angew. Chem. Int. Ed.* **2012**, *51*, 5147–5151; *Angew. Chem.* **2012**, *124*, 5237–5241.
[32] M. A. Sk, S. Manzhos, *J. Power Sources* **2016**, *324*, 572–581.
[33] S. Renault, V. A. Oltean, C. M. Araujo, A. Grigoriev, K. Edstrom, D. Brandell, *Chem. Mater.* **2016**, *28*, 1920–1926.
[34] L. Wang, Z. Schnepp, M. M. Titirici, *J. Mater. Chem. A* **2013**, *1*, 5269–5273.
[35] L. Wang, J. Xue, B. Gao, P. Gao, C. Mou, J. Li, *RSC Adv.* **2014**, *4*, 64744–64746.
[36] P. Gao, L. Wang, Y. Zhang, Y. Huang, K. Liu, *ACS Nano* **2015**, *9*, 11296–11301.
[37] H. Wang, S. Yuan, Z. Si, X. Zhang, *Energy Environ. Sci.* **2015**, *8*, 3160–3165.
[38] G. Li, H. Yang, F. Cheng, W. Shi, J. Chen, P. Cheng, *Inorg. Chem.* **2016**, *55*, 4935–4940.

Received: July 13, 2016
Revised: September 27, 2016
Published online on January 4, 2017